KINETICS AND MECHANISMS OF METAL RETENTION / RELEASE IN GEOCHEMICAL PROCESSES IN SOIL

PROGRESS REPORT (9TH MONTH)

Submitted to

Dr. Paula Davidson

GEOSCIENCES RESEARCH PROGRAM, OFFICE OF BASIC ENERGY SCIENCES, OFFICE OF ENERGY RESEARCH

DOE

by

Robert W. Taylor

Principal Investigator and Professor of Soil/Environmental Chemistry

ALABAMA A&M UNIVERSITY

May 1997

PROGRESS REPORT

Kinetics and Mechanisms of Metal Retention/Release in Geochemical Processes in Soil

Award # DE-FG07-96ER14718

PI: Robert W. Taylor

Institution: Alabama A&M University

1. New projects at the National Synchrotron Light Source, Brookhaven National Laboratory: We were awarded 12 days on a new NSLS project (#3235) dedicated to extended x-ray absorption fine-structure (EXAFS) studies of ion adsorption at mineral surfaces. This brings the number of active projects at NSLS to two. The other project (#1694), which has 16 days remaining out of the original assignment of 30 days, is dedicated to X-ray absorption near-edge structure (XANES) studies of oxidation and reduction processes in soils.

2. Ton clustering and dispersal at the mineral/ water Interface: We are currently studying the competing tendencies of ion dispersal, resulting in surface complexation of ions at isolated sites on mineral surfaces, and ion clustering or surface precipitation. Copper (II) shows a tendency to form surface precipitates on silica surfaces (Xia et al., 1997) while it favors dispersal on aluminum oxide surfaces (Weesner et al., submitted).

   EXAFS provides solid evidence of surface precipitation when the majority of the adsorbed metal ion is in a precipitated state, but is not very sensitive to clustering if it involves a relatively small population of the adsorbed ions. We have recently used a SQUID magnetometer to measure the effective magneton number of Cu(II) adsorbed on boehmite. These measurements clearly indicate

that dispersed Cu(II) ions populate the boehmite/ water interface up to coverages approaching 45% of a monolayer with negligible antiferromagnetic ordering characteristic of copper hydroxide precipitates. Furthermore, we have successfully measured the effective magneton number of adsorbed Cu(II) at coverages as low as 0.2 micromole per meter square, equivalent to 4% monolayer coverage of hydrated ions.

3. Adsorption of chromate by goethite and boehmite: We have completed data collection on a study comparing the mechanism of chromate anion adsorption by two oxyhydroxide minerals found in soils: the iron oxyhydroxide goethite and the aluminum oxyhydroxide boehmite. Our preliminary analysis of EXAFS results clearly indicate differences in chromate adsorption on the two oxyhydroxides, suggesting as single population of adsorption sites on boehmite and at least two population of sites on goethite. A recent EXAFS study (Fendorf et 1., 1997) claims chromate surface coverages ranging up to 7.95 micromole per meter square, but our study fails to achieve coverages of that magnitude. In fact, the maximal chromate surface coverages of 2.2 micromole chromate per meter square on goethite are quite close to-maximal surface coverages of phosphate on similar oxide surfaces (Bleam et al., 1991). Our data include IR spectra of chromate adsorbed to titania, boehmite and goethite which confirm our XANES results regarding chromate symmetry in the adsorbed state.

4. Nickel(II) adsorption by boehmite: We will collect both magnetic susceptibility and x-ray absorption data on Ni(II) adsorbed to boehmite during July 1997. The primary objective of this first round of adsorption studies will be to measure the dispersal of Ni(II) by monitoring the effective magneton number as a function of Ni(ll) surface coverage. We will supplement these magnetic measurements

with and EXAFS study of Ni(II) adsorption. The results of our Ni(II) adsorption study are scheduled for presentation at the October 1997 annual meetings of the Soil Science Society of America in Anaheim, CA.

5. Lead retention in smectite was investigated by equilibrium studies, coupled with spectroscopic methods. The isotherm and pH-edge of lead adsorption were measured by batch experiments. FTIR and XRD spectroscopies indicated various lead complexes on the clay surfaces and interlayers at different lead concentration and pH.

Lead retention in smectite is a fast reaction as the retention reached equilibrium in minutes. As shown in Figure 1, almost all the Pb adsorbed in the smectite was adsorbed within 0.1 hour. After that the retention kinetics exhibited a flat line. Therefore, four days were adequate time for equilibrium conditions used for pH-edge and isotherm studies.

The isotherm of lead retention in the smectite (Figure 2) showed L-shape and can be fitted with Langmuir equation:

$$S = \frac{KbC}{(1+KC)} \qquad \frac{C}{S} = \frac{1}{Kb} + \frac{C}{b}$$

where S is the amount of Pb adsorbed in the smectite (mmol kg^{-1}). C is Pb concentration in the solution (mmol L-r), K is a reaction coefficient, and b is the maximum retention of Pb in the smectite. The goodness-of-fit (r^2) was 0.995 and the fitting parameters were 0.932 for K and 400.7 mmol kg^{-1} for *b*.

In the range of solution concentrations from 0.5 to 2 mM, Pb retention in the smectite was almost linear (Figure 3). The slope of the retention isotherms increased with increasing pH. When pH was above 6.4, the isotherm slopes remained similar.

The pH-adsorption edges for lead retention in the smectite is presented in Figure 4. At the same ionic strength (10 mM), the percentage of lead adsorbed in the smectite increased with decreasing Pb concentration in solutions for the pH below Pb hydrolysis point. At the same concentration of solution lead (2 mM), increasing ionic strength from 10 mM to 50 mM decreased lead retention about half at the pH below Pb hydrolysis point.

Infrared Spectroscopy

Presented in Figure 5, 6 and 7 are FTIR spectra of lead treated smectite samples from pH adsorption edge study. For the pH adsorption edge with 0.5 mM lead nitrate solutions, a weak peak with maximums near 1406 cm^{-1} was observed in the spectra for Pb adsorbed at low pH. The peak became more intensive and shifted to a lower wavenumber as pH increased (Figure 5). When lead concentrations increased to 1 mM and even to 2 mM, this broad and intense peak with a maximum near 1398 cm-i was observed in the spectra for Pb adsorbed at pH > 6.4 in Figure 6 and pH > 5.6 in Figure 7. At Pb concentration of 2 mM, a shoulder centered near 1470 cm^{-1} was exhibited clearly at this broad and intensive peak (Figure 7). Therefore, the peak may be composed of several IR bands, including an OH bending band from lead hydroxides and a CO_3^{2-} asymmetric stretching band. Further curve fitting is needed to deconvolute this combination peak.

Shown in Figure 8 and 9 are FTIR spectra of lead retention isotherms. When the smectite was allowed to react with lead nitrate solutions of various concentrations, the equilibrium pH averaged at pH 5.6 with a range from pH 6.2 for 0.01 mM $Pb(NO_3)_2$ solution to pH 5.2 for 20 mM $Pb(NO_3)_2$ solution. The peak centered near 1398 cm^{-1} was weak until the lead concentration reached 20 mM (Figure 8). When the reaction mixture was titrated to near pH 5.6, the peak centered near 1398 cm^{-1} was significant as the lead concentration reached 2 mM (Figure 9).

Siantar and Fripiat (1995) used lead perchlorate at average pH 5.5 while we used lead nitrate in this study. Lead perchlorate gives the hydrated ion Pb^{2+} while lead nitrate gives $PbNO_3^+$ in solutions (Harrison et al., 1983). The IR peaks observed were within both carbonate, nitrate and hydroxide ranges.

X-ray Diffraction Spectroscopy

The basal spacing of the smectite before and after treatment with different lead nitrate solutions was determined by x-ray diffraction (XRD). Shown in Figure 10 and 12 are the d-spacing of the smectite treated with $Pb(NO_3)_2$ at different pH. Comparison among the basal spacings of the lead-treated smectite at different pH shows that the $d001$ spacings increase with the decrease of pH (Table 1). The d-spacing of the smectite with Pb adsorbed at pH 8.8 (about 12.4 Å) was similar to that of the Na-saturated clay (12.5 Å). The d-spacing of Pb-treated smectite increased to about 12.7 Å for the samples in the range of pH 4.3 to pH 6.3. When the pH was below 3.3, the d-spacing of Pb-treated smectite increased with decreasing pH and reached an average of 13.4 Å at pH 2.4.

Comparison between the basal spacing of untreated smectite (Na-saturated) and Pb-treated smectite in the retention isotherm (average pH 5.6) was shown in Figure 12. The basal spacing of the smectite treated with lead solutions below 2 mM $Pb(NO_3)_2$ was similar to that of untreated smectite (Na-saturated) with a small variation (12.5 - 12.7 Å). When the lead concentration in solutions increased above 2 mM, the d-spacing of Pb-treated smectite increased with increasing Pb concentration (Table 2) though the amount of Pb retention in smectite changed little (Figure 2).

The change in basal spacing for the Pb-treated smectite is helpful to study whether any metal hydroxides formed in the interlayers of the clay. The d-spacing increase of Pb-treated smectite in the mid pH range may be the results of Pb hydroxide intercalations into the smectite interlayers. A possible explanation of the

d-spacing increase for Pb-treated smectite at pH below 3.3 could be aluminum dissolution and Al hydroxides re-precipitation in the interlayers of the smectite at low pH.

REFERENCES

Allison, J. D., **Brown,** D. S. and K. J. Novo-Gradac. 1991. MINTEQA2/ PRODEFA2, A geochemical assessment mode1 for environmental systems: version 3.0 user's manual. EPA/ 600/ 3-91/ 021.

Arnfalk, P., Wasay, S. A. and S. Tokunaga. 1996. A comparative study of Cd, Cr(III), Cr(VI), Hg, and Pb uptake by minerals and soil minerals. Water, Air, and Soil Pollution 87:131-148.

Bleam, W. F., Pfeffer, P. E., Goldberg, S., Taylor, R. W., Dudley, R., 1991, A P-31 solid-state nuclear magnetic resonance study of phosphate adsorption at the boehmite/ aqueous solution interface, Langmuir, 7:1702-1712.

Fendorf, S. E., Eick, M. J., Grossl, P., Sparks, D. L., 1997, Arsenate and chromate retention mechanisms on goethite. 1. Surface structure, Environ. Sci. Technol. 31:315-319.

Gan, H., Bailey, G. W. and Y. S. Yu. 1996. Morphology of lead(II) and chromium(III) reaction products on phyllosilicate surfaces as determined by atomic force microscopy. Clay & Clay Miner. 44:734-743.

Harrison, P. G., Healy, M. A. and A, T. Steel. 1983. Lead-207 chemical shift data for bivalent lead compounds: Thermodynamics of the equilibrium in aqueous solution in the temperature range 303 - 323 K. J. Chem. Soc. Dalton Trans. 1845-1848.

Majone, M. Papini, M. P. and E. Rolle. Modeling lead adsorption on clays by models with and without electrostatic terms. J Colloid & Interface Sci. 179:412-425.

Reed, B. E. and S. R. Cline. 1994. Retention and release of lead by a very fine sandy loam. I. isotherm modeling. Separation Sci. & Tech. 29:1529-1551.

Siantar, D. P., Feinberg, B. and J. J Fripiat. 1994. Interaction between organic and inorganic pollutants in the clay interlayer. Clay & Clay Miner. 42:187-196.

Siantar, D. P. and J. J Fripiat. 1995. Lead retention and complexation in a magnesium smectite (hectorite). J Colloid & Interface Sci. 169;400-407.

Weesner, F. J., Bleam, W. F., X-ray absorption and EPR spectroscopic characterization of adsorbed Cu(II) complexes at the boehmite surface, J. Colloid Interface Sci., submitted.

Xia, K., Mehadi, A., Taylor, R. W., Bleam, W. F., 1997, X-ray absorption and electron paramagnetic resonance studies of Cu(II) sorbed on silica: Surface-induced precipitation at low surface coverages, J. Colloid Interface Sci., 185:252-257.

LIST OF FIGURE CAPTIONS

Figure 1. Kinetic process of Pb retention in smectite SWy-2 from 2 mM lead nitrate solution.

Figure 2. Retention isotherm of Pb in smectite SWy-2 from lead nitrate solutions ranging from 0.01 mM to 20 mM $Pb(NO_3)_2$ in 10 mM $NaNO_3$.

Figure 3. Retention isotherm of Pb in smectite SWy-2 from lead nitrate solutions ranging from 0.5 mM to 2 mM $Pb(NO_3)_2$ in 10 mM $NaNO_3$ at different pH.

Figure 4. pH adsorption edges (Pb retention in smectite SWy-2 from lead nitrate solutions at different pH).

Figure 5. FTIR spectra of SWy-2 with Pb adsorbed from 0.5 mM lead nitrate solutions at different pH.

Figure 6. FTIR spectra of SWy-2 with Pb adsorbed from 1 mM lead nitrate solutions at different pH.

Figure 7. FTIR spectra of SWy-2 with Pb adsorbed from 2 mM lead nitrate solutions at different pH.

Figure 8. FTIR spectra of SWy-2 with Pb adsorbed from 0.01 mM to 20 mM lead nitrate solutions at average pH 5.6.

Figure 9. FTIR spectra of SWy-2 with Pb adsorbed from 0.01 mM to 2 mM lead nitrate solutions titrated to pH 5.6

Figure 10. The basal spacing, $d001$(Å), of the smectite treated with 1 mM lead nitrate solutions at different pH.

Figure 11. The basal spacing, $d001$(Å), of the smectite treated with 2 mM lead nitrate solutions at different pH.

Figure 12. The basal spacing, $d001$(Å), of the smectite treated with 0.01 mM to 20 mM lead nitrate solutions at average pH 5.6.

Table 1. The basal spacing, $d(001)$(Å), of the smectite treated with Pb nitrate at different pH

	pH 2.5	pH 3.3	pH 4.3	pH 5.2	pH 5.6	pH 6.4	pH 7.2	pH 8.6
1 mM Pb	13.5	12.7	12.6	12.5	12.7	12.4	12.3	12.3
2 mM Pb	13.3	12.9	12.8	12.7	12.7	12.8	12.6	12.4

Table 2. The basal spacing, $d(001)$(Å), of the smectite treated with increasing concentrations of lead nitrate

Pb nitrate concentration	basal spacing, $d(001)$(Å),
0.01 mM	12.7
0.05 mM	12.5
0.1 mM	12.7
0.5 mM	12.5
1.0 mM	12.5
2.0 mM	12.6
5.0 mM	12.9
10 mM	13
20 mM	13.4

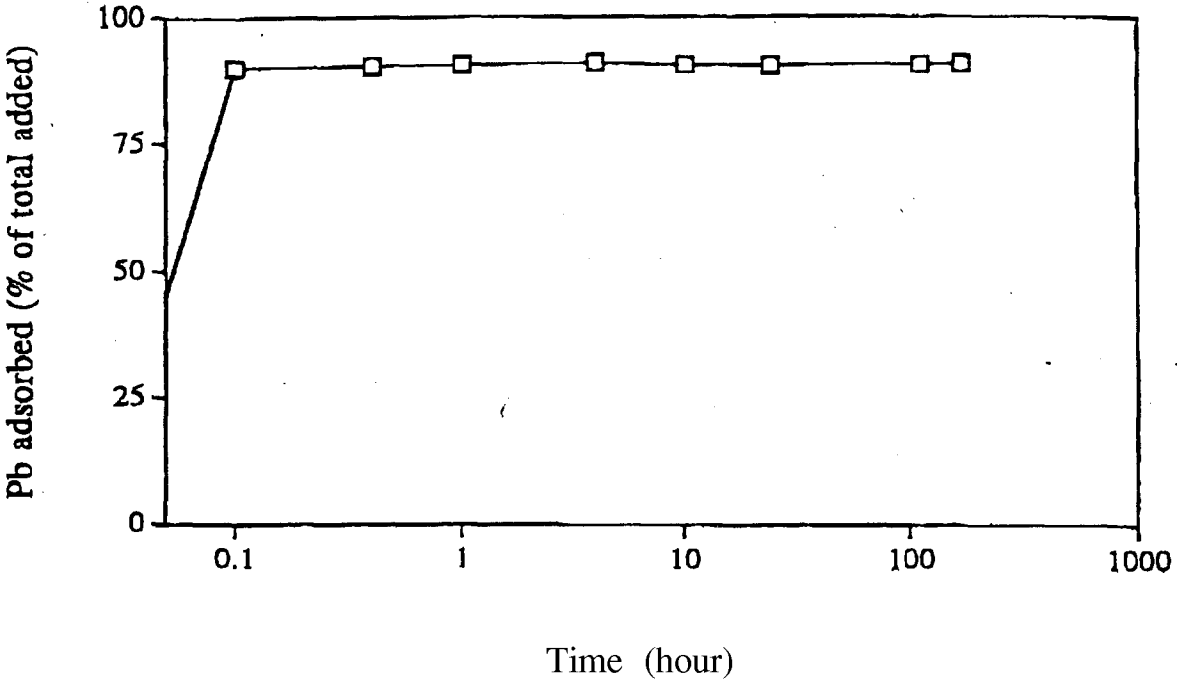

Figure 1. Kinetics of Pb retention in smectite from 2 mM lead nitrate solution (pH 5.5)

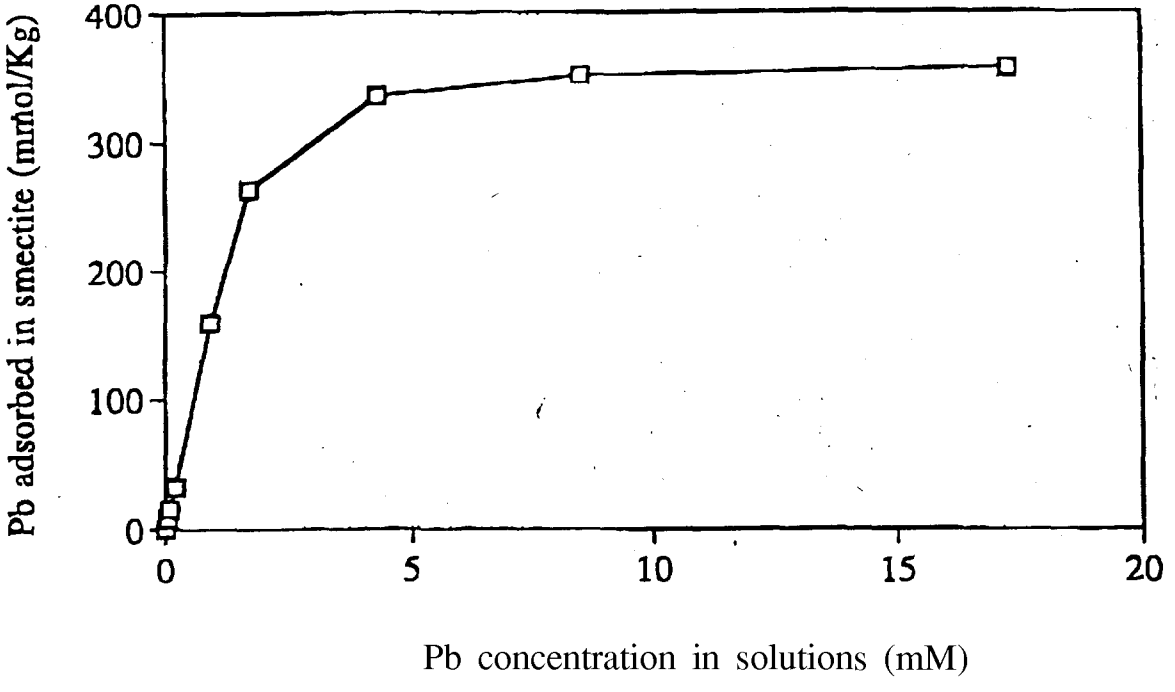

Figure 2. Retention isotherm of Pb in smectite from lead nitrate solutions (average pH 5,6)

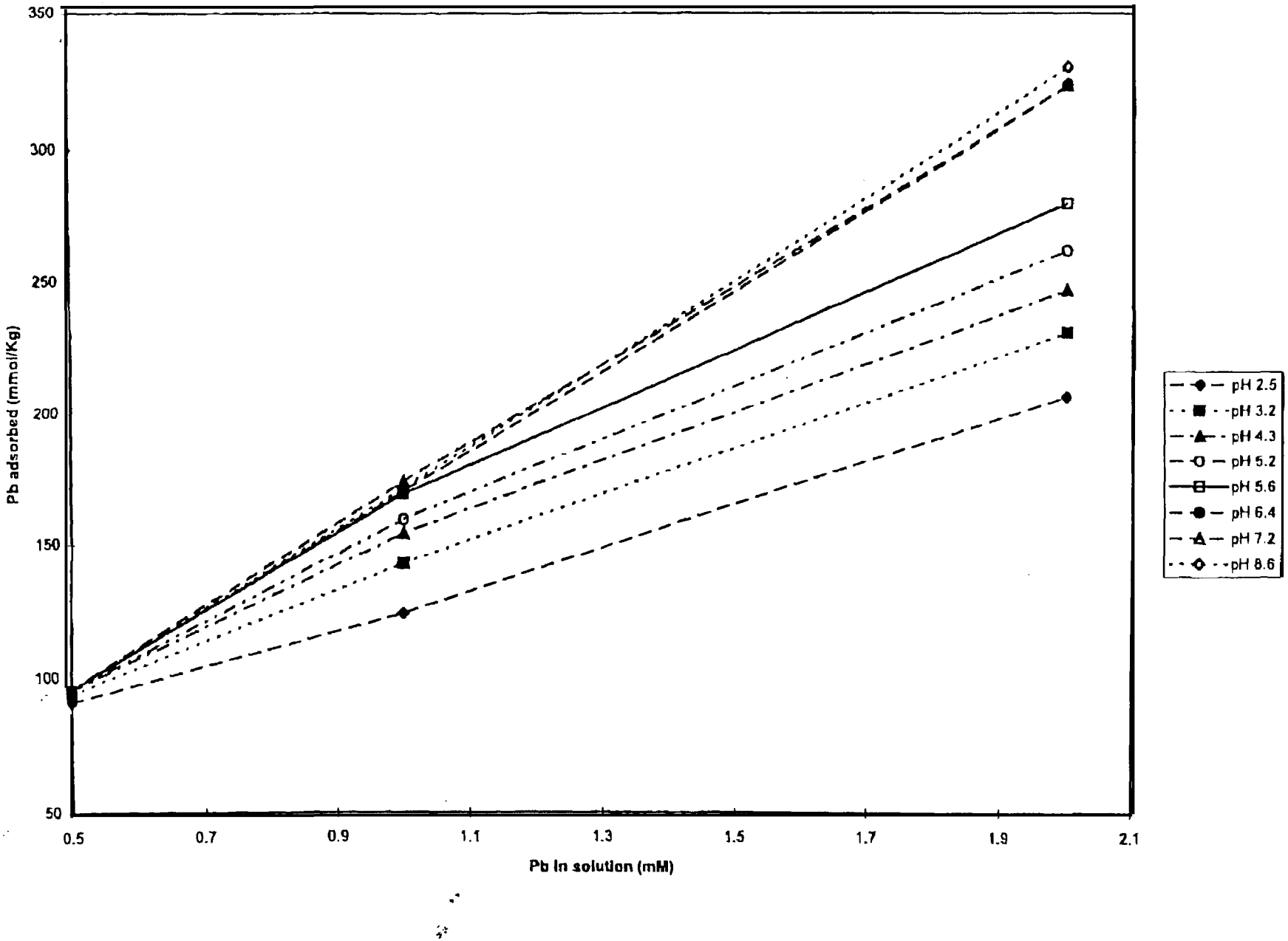

Figure 3. Retention isotherm of Pb in smectite from lead nitrate solutions ranging from 0.5 mM to 2 mM Pb at different pH

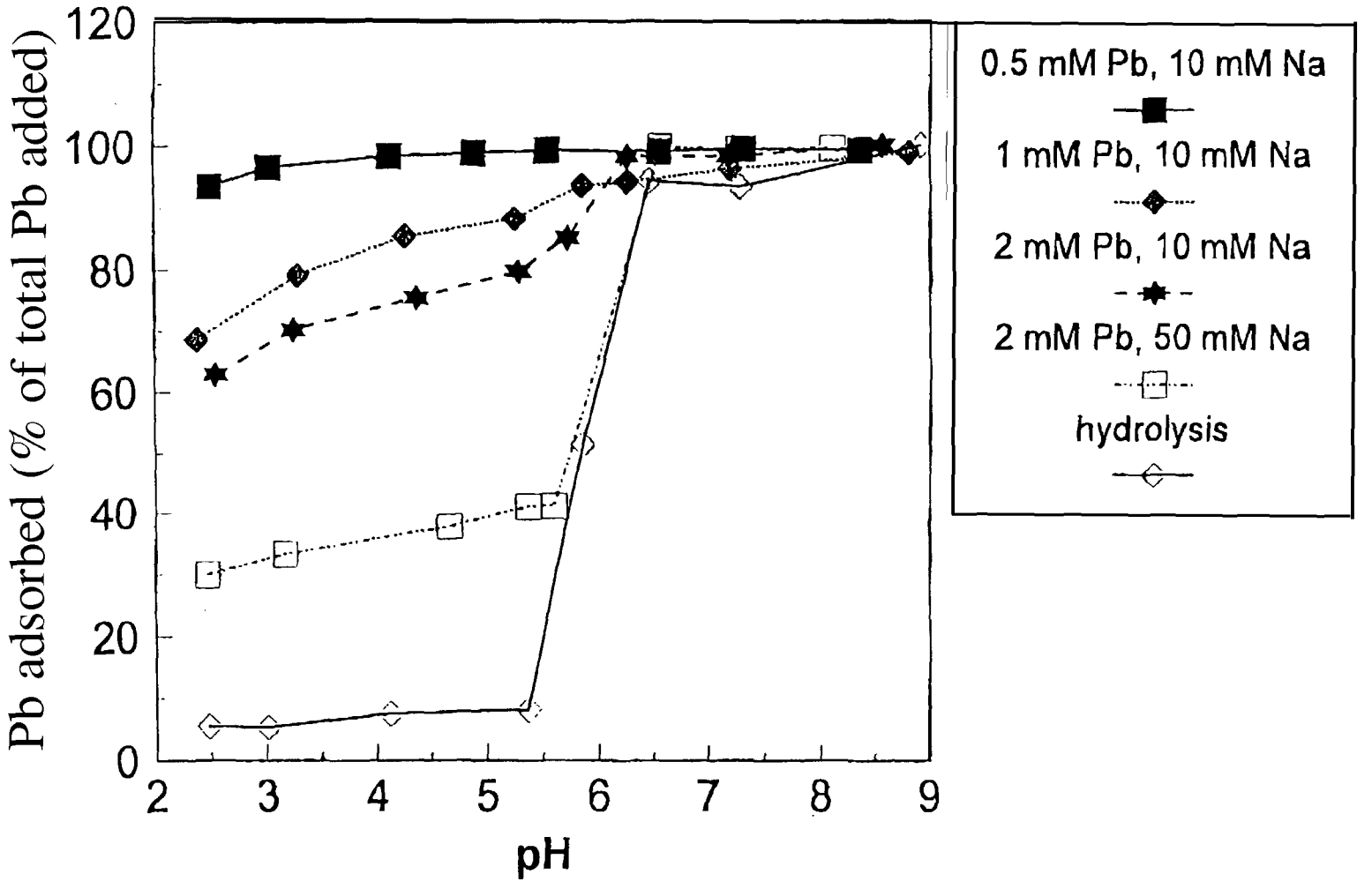

Figure 4. pH adsorption edge (Pb retention in smectite from lead nitrate solutions at different pH)

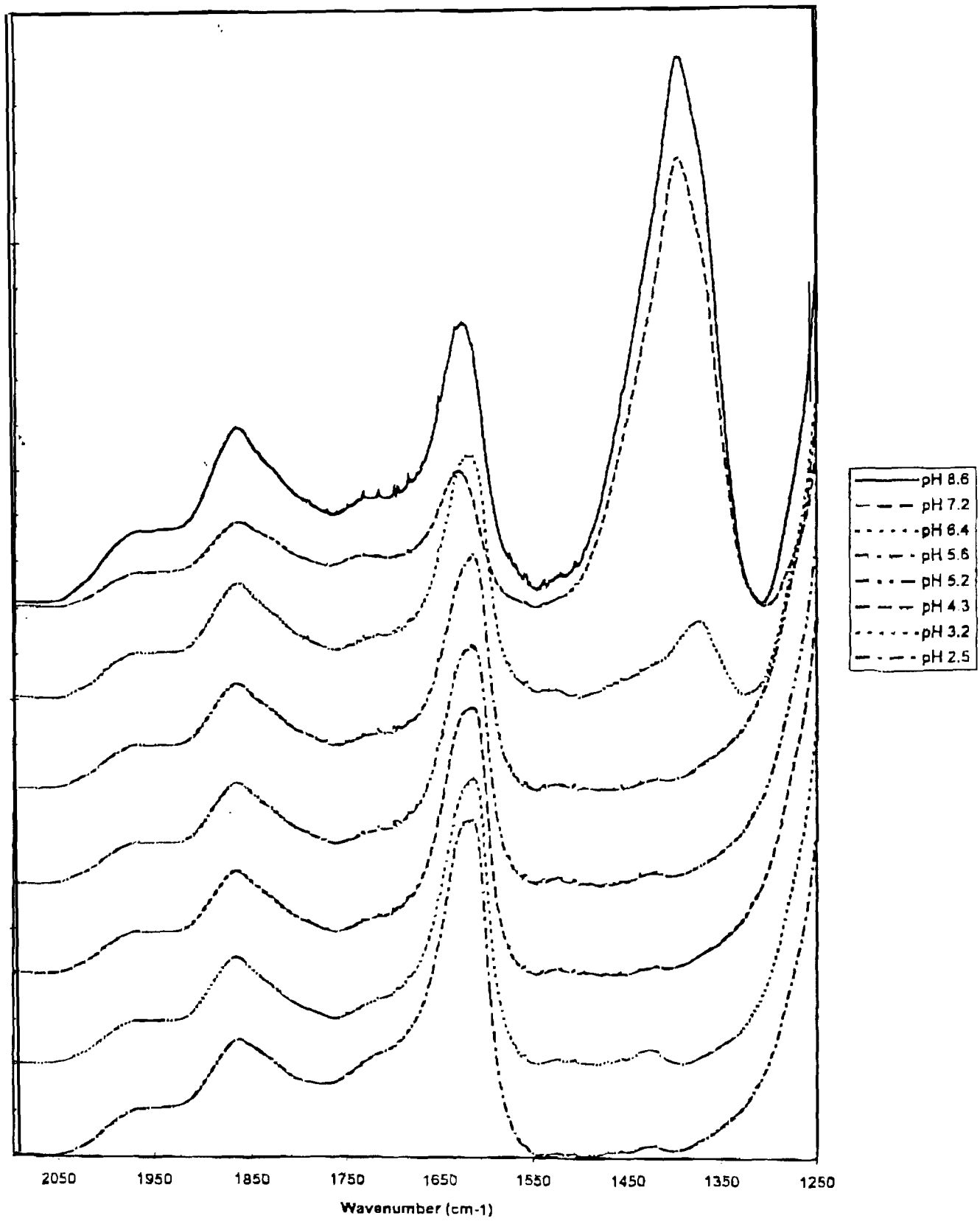

Figure 6. FTIR spectra of SWy-2 with Pb adsorbed from 1 mM lead nitrate solutions at different pH

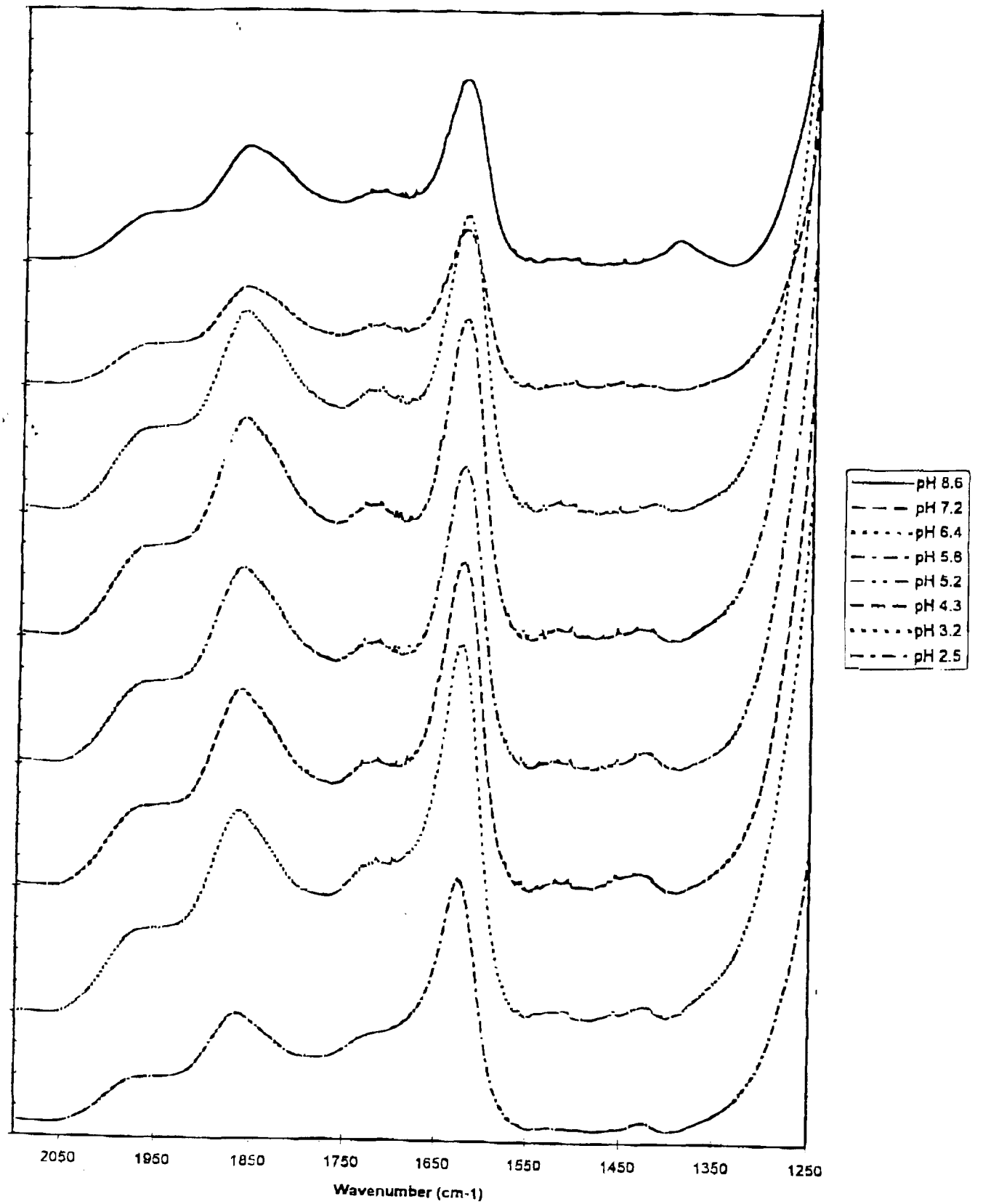

Figure 5. FTIR spectra of SWy-2 with Pb adsorbed from 0.5 mM lead nitrate solutions at different pH

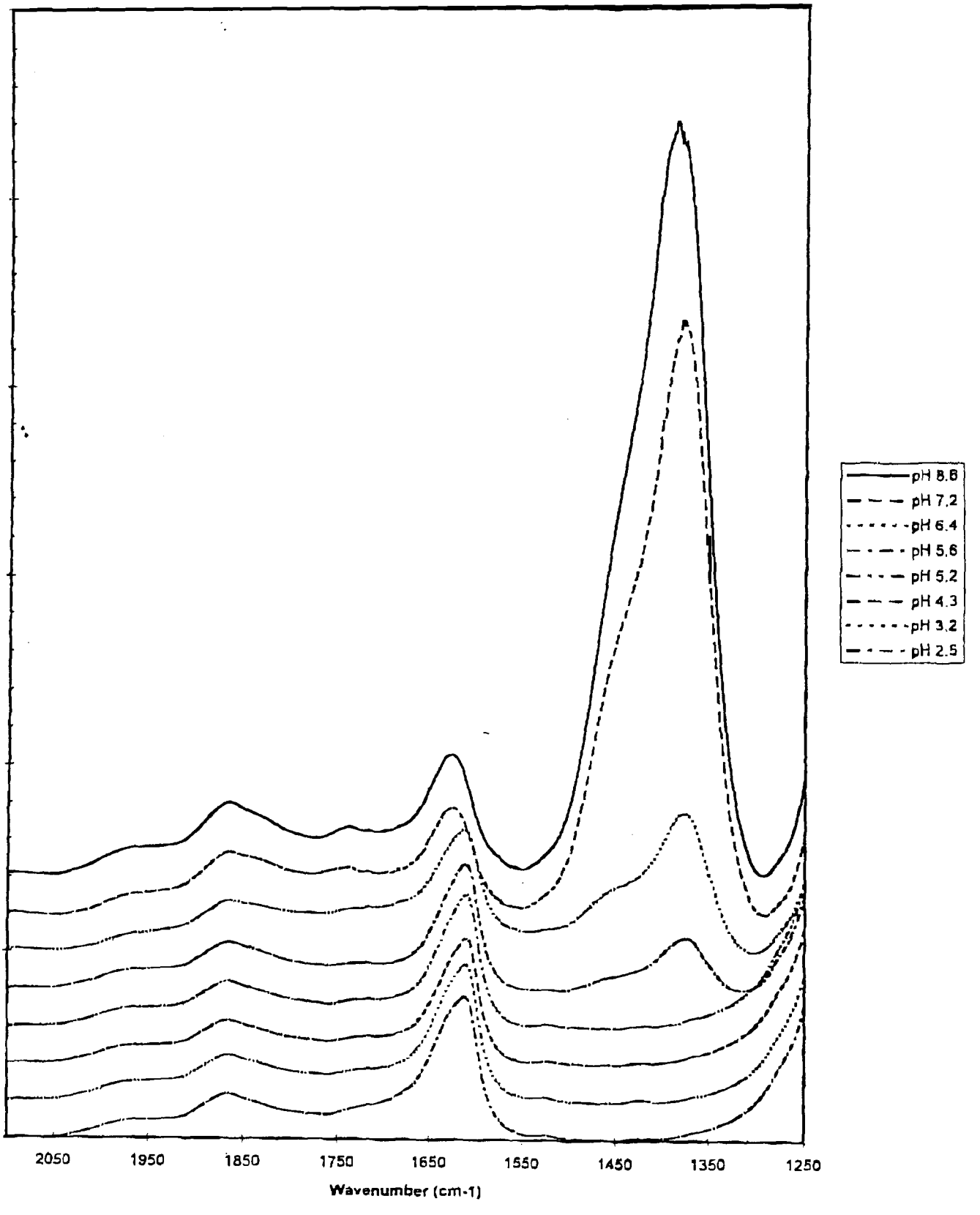

Figure 7. FTIR spectra of SWy-2 with Pb adsorbed from 2 mM lead nitrate solutions at different pH

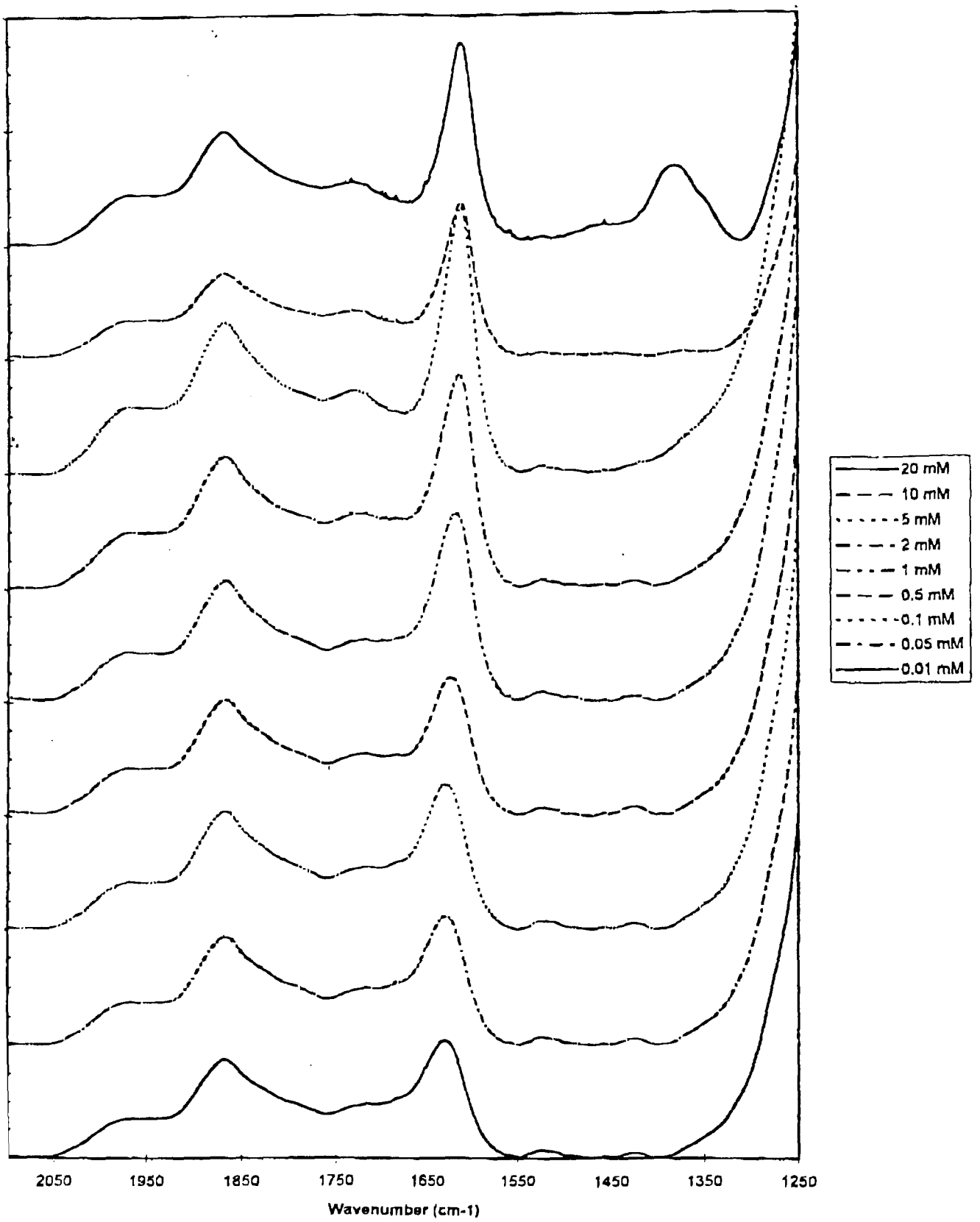

Figure 8. FTIR spectra of SWy-2 with Pb adsorbed from 0.01 mM to 20 mM Pb nitrate solutions at average pH 5.6

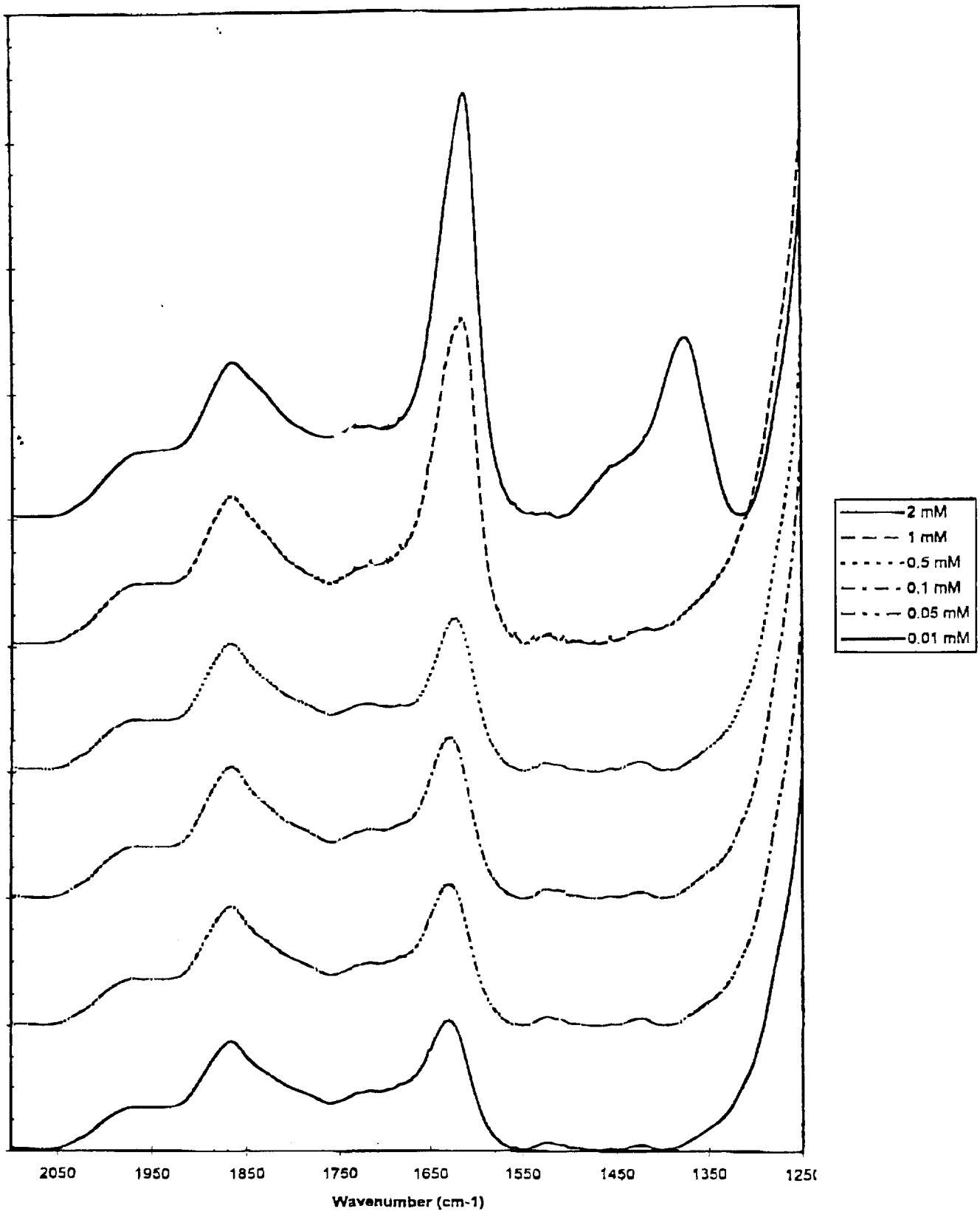

Figure 9. FTIR spectra of SWy-2 with Pb adsorbed from 0.01 mM to 2 mM Pb nitrate solutions titrated to pH 5.6

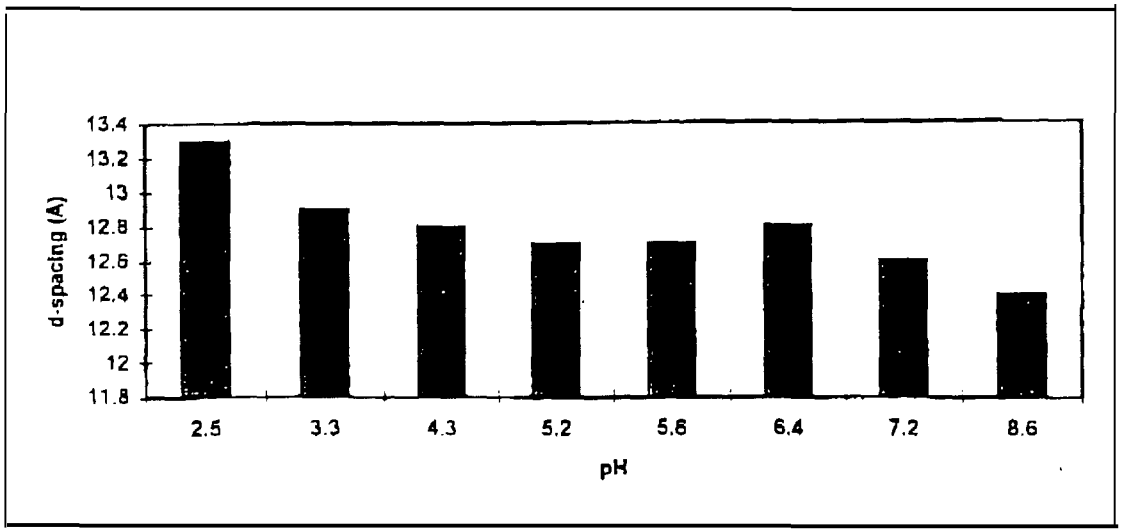

Figure 10. The basal spacing, d001(Å), of the smectite treated with 1 mM lead nitrate solutions at different pH.

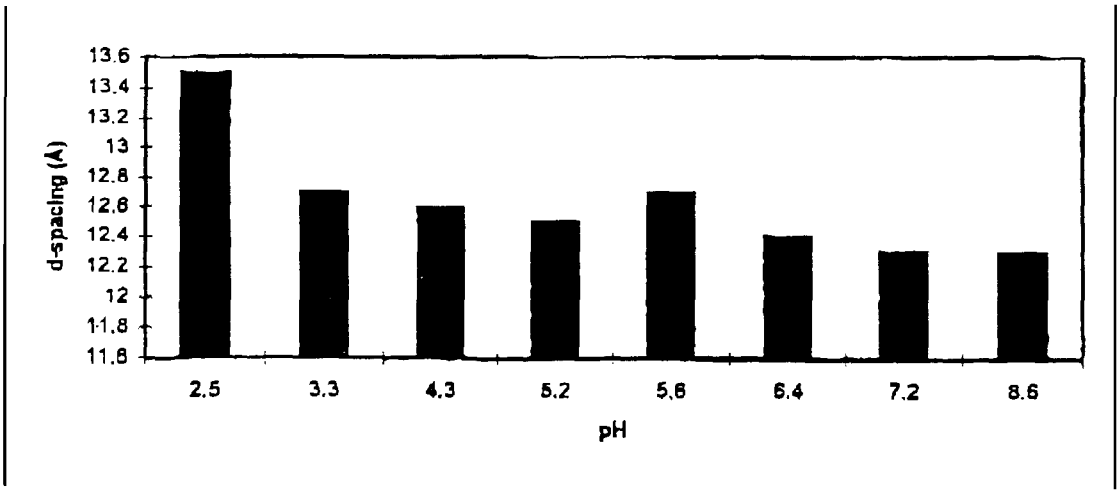

Figure 11. The basal spacing, d001(Å), of the smectite treated with 2 mM lead nitrate solutions at different pH.

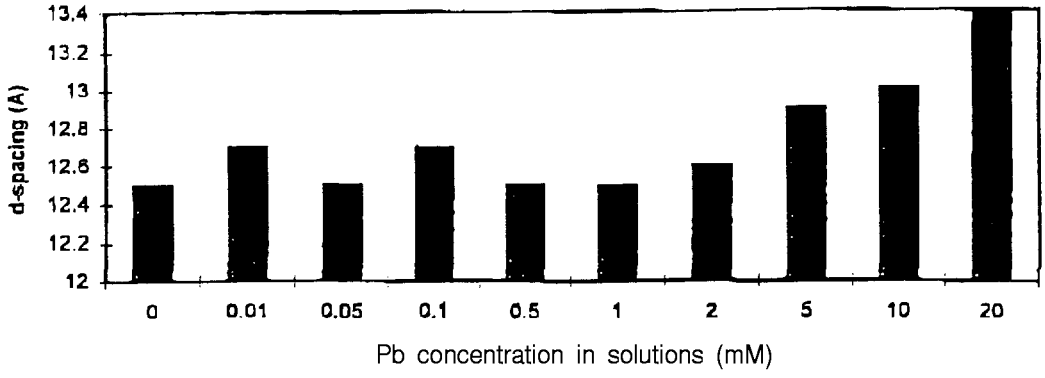

Figure 12. The basal spacing, d001(Å), of the smectite treated with 0.01 mM to 20 mM lead nitrate solutions at average pH 5.6.

PURCHASING SYSTEM

ACCOUNT-CODE BUDGET MANAGER S REPORT 05/29/97 PAGE 01 OF 02

2-202-14-3150 KINETICS AND MERCHANISM BUDGET MGR : DR ROBERT TAYLOR
BEG-DATE : 10/01/96 END-DATE : 09/14/99 66 % OF TIME

OBJ	DESC	BUDGETED	EXPENDED	ENCUMBERED	BALANCE	%XP
105	PRINCIPAL	20,000.00	.00	.00	20,000.00	00
140	GRADUATE A	.00	.00	.00	.00	00
150	WAGES - ST	2,785.00	2,011.62	.00	773.38	72
220	SOCIAL SEC	1,530.00	.00	.00	1,530.00	00
225	RETIREMENT	1,846.00	.00	.00	1,846.00	00
230	GROUP INSU	112.00	.00	.00	112.00	00
240	GROUP INSU	668.00	.00	.00	668.00	00
260	UNEMPLOYME	600.00	.00	.00	600.00	00
270	WORKERS CO	116.00	.00	.00	116.00	00
330	OFFICE SUP	.00	.00	.00	.00	00
390	OTHER SUPP	9,135.00	3,813.31	4,231.06	1,090.63	88
460	TRAVEL	4,000.00	1,759.90	745.00	1,495.10	62
585	OTHER CONT	20,250.00	20,205.00	.00	45.00	99
590	COMPUTER S	.00	.00	.00	.00	00

PRESS PF1 = FWD, PF2 = BWD, PF3 = REQ. PA1 = ANOTHER ACT NUM. PA2 = MENU SCREEN

PURCHASING SYSTEM

ACCOUNT-CODE BUDGET MANAGER S REPORT 05/29/97 PAGE 02 OF 02

2-202-14-3150 KINETICS AND MERCHANISM BUDGET MGR : DR ROBERT TAYLOR
BEG-DATE : 10/01/96 END-DATE : 09/14/99 66 % OF TIME

OBJ	DESC	BUDGETED	EXPENDED	ENCUMBERED	BALANCE	%XP
620	LEGAL. CON	10,000.00	10,000.00	.00	.00	100
790	INDIRECT C	18,470.00	4,188.77	.00	14,281.23	22
820	FURNITURE	60,000.00	.00	.00	60,000.00	00
830	BOOKS	.00	.00	.00	.00	00
	TOTALS >	149,512.00	41,978.60	4,976.06	102,557.34	31

PRESS PF1 = FWD, PF2 = BWD, PF3 = REQ. PA1= ANOTHER ACT NUM, PA2 = MENU SCREEN

PURCHASING SYSTEM

ACCOUNT-CODE BUDGET MANAGER S REPORT 05/29/97 PAGE 01 OF 02

2-202-14-3150 KINETICS AND MERCHANISM BUDGET MGR : DR ROBERT TAYLOR
BEG-DATE : 10/01/96 END-DATE : 09/14/99 66 % OF TIME

OBJ	DESC	REQUISITIONS	BAL-INCL-REQS	STS
105	PRINCIPAL	.00	20,000.00	A
140	GRADUATE A	.00	.00	A
150	WAGES - ST	.00	773.38	A
220	SOCIAL SEC	.00	1,530.00	A
225	RETIREMENT	.00	1,846.00	A
230	GROUP INSU	.00	112.00	A
240	GROUP INSU	.00	668.00	A
260	UNEMPLOYME	.00	600.00	A
270	WORKERS CO	.00	116.00	A
330	OFFICE SUP	.00	.00	A
390	OTHER SUPP	177.34	913.29	A
460	TRAVEL	.00	1,495.10	A
585	OTHER CONT	.00	45.00	A
590	COMPUTER S	.00	.00	A

PRESS PF1 = FWD, PF2 = BWD. PF3 = REQ. PA1 = ANOTHER ACT NUM. PA2 = MENU SCREEN

Budget Projection for FYI
(through August 31, 1997)

By the end of FYI I expect to have the following expenditures:

a) Equipment	-	$60,000 for FIIR Instrument
b) PI Salary	-	19,744.78
c) Supplies	-	1,090.63
d) Indirect Cost	-	10,281.23
	Total	91,116.41

The present balance is 102,557.34 and with an expenditures of $91,116.41 by August 31, 1997. I expect to have a balance of $11,440.93.